NAVAL SHIP RESEARCH AND DEVELOPMENT CENTER
Bethesda, Md. 20034

A TWO-DEGREE-OF-FREEDOM MODEL FOR THE TWO-DIMENSIONAL DYNAMIC MOTIONS OF SUSPENDED EXTENSIBLE CABLE SYSTEMS

by

Henry T. Wang

APPROVED FOR PUBLIC RELEASE;
DISTRIBUTION UNLIMITED

SHIP PERFORMANCE DEPARTMENT
RESEARCH AND DEVELOPMENT REPORT

October 1971

Report 3663

Report 3663

A TWO-DEGREE-OF-FREEDOM MODEL FOR THE TWO-DIMENSIONAL DYNAMIC MOTIONS OF SUSPENDED EXTENSIBLE CABLE SYSTEMS

The Naval Ship Research and Development Center is a U. S. Navy center for laboratory effort directed at achieving improved sea and air vehicles. It was formed in March 1967 by merging the David Taylor Model Basin at Carderock, Maryland with the Marine Engineering Laboratory at Annapolis, Maryland. The Mine Defense Laboratory (now Naval Ship R & D Laboratory) Panama City, Florida became part of the Center in November 1967.

Naval Ship Research and Development Center

Bethesda, Md. 20034

MAJOR NSRDC ORGANIZATIONAL COMPONENTS

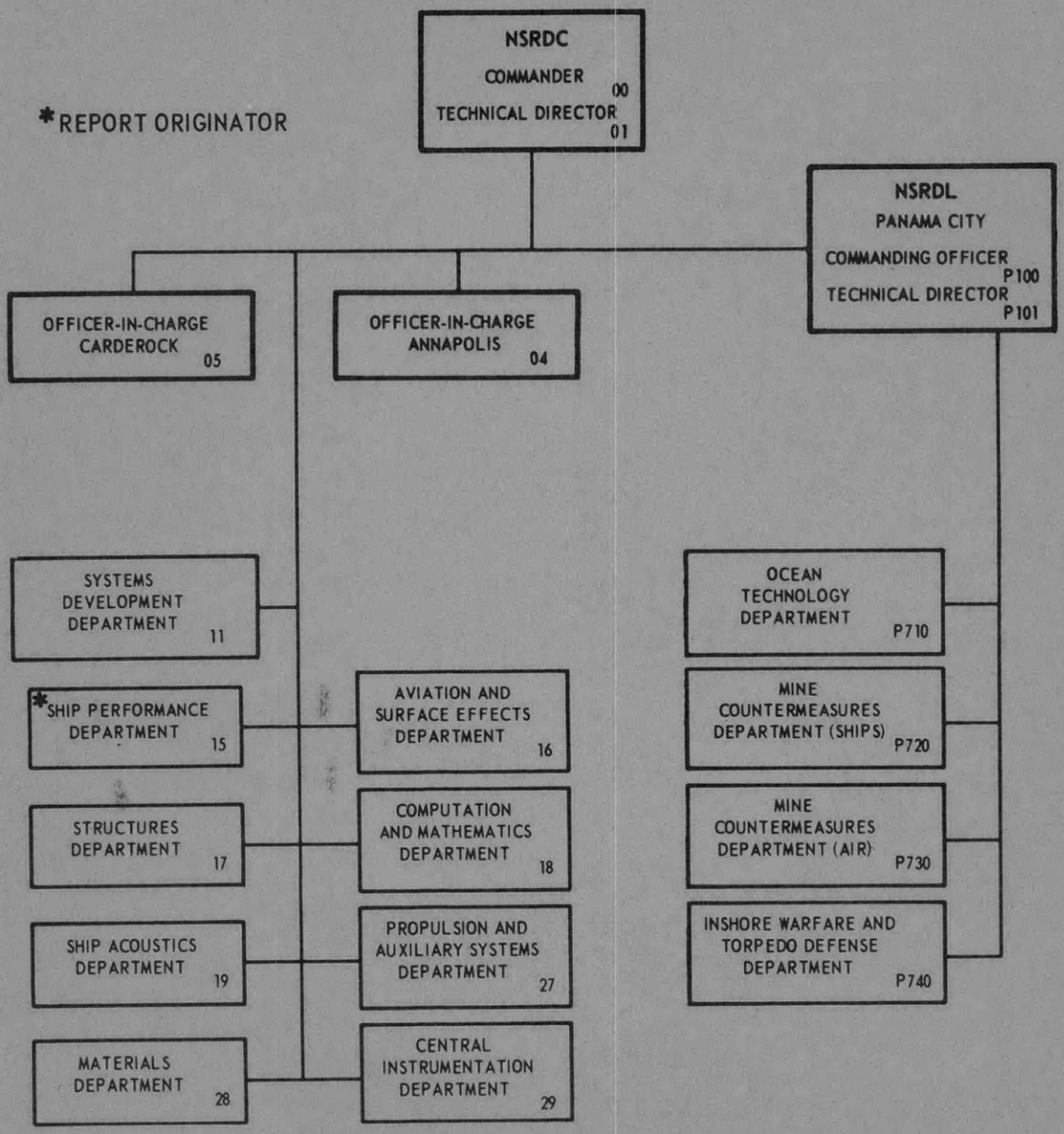

NDW-NSRDC 3960/43 (3-70)

DEPARTMENT OF THE NAVY
NAVAL SHIP RESEARCH AND DEVELOPMENT CENTER
BETHESDA, MD. 20034

A TWO-DEGREE-OF-FREEDOM MODEL FOR THE TWO-DIMENSIONAL DYNAMIC MOTIONS OF SUSPENDED EXTENSIBLE CABLE SYSTEMS

by

Henry T. Wang

October 1971

Report 3663

TABLE OF CONTENTS

LIST OF FIGURES

LIST OF TABLES

NOTATION

A	Area of cable cross section
a	Ocean wave amplitude
C	Damping or resistance coefficient
$C_D A_b$	Drag area of lower body
c	Steady horizontal fluid flow relative to cable
D	Drag
d	Cable thickness
E	Modulus of elasticity
e	Cable strain = u/ℓ_r
F	Force
f	Frequency in hertz
g	Gravity constant
i	$\sqrt{-1}$
K	Kinetic energy
k	Spring constant = $(AE)_r/\ell_r$
L	Lagrangian function = K - V
ℓ	Cable length
M	Mass
m	Mass per unit length
N	Number of cable segments
n	$2\pi / \lambda$
p	Poisson's ratio
Q	Damping or resistance force
s	Distance measured along the cable
T	Cable tension
t	Time
u	Cable stretch at the lower body
u_1	du/dt
V	Potential energy

v	Velocity
W	Weight in water
w	Stretch along the cable
x	Horizontal coordinate positive to the right
y	Vertical coordinate positive downwards
γ	Added mass factor
$\dot{\eta}$	Ocean velocity in the y direction
λ	Ocean wave length
$\dot{\xi}$	Ocean velocity in the x direction
ρ	Fluid density
σ	$\sqrt{2\pi\ g/\lambda}$
ϕ	Angle of the cable with the vertical
ϕ_l	$d\phi/dt$
ω	$2\pi\ f$
ω_n	Natural frequency for horizontal motions of the cable in radians/second

Subscripts

A	Amplitude
b	Lower body
c	Cable
D	Drag
e	Strain energy
f	Fluid
g	Gravity
I	Internal damping
i	Cable segment index
n	Normal
o	Zero tension
p	Pendulum motion
q	Relative to cable
r	Reference tension

s	Ocean surface
t	Tangential
u	Cable stretch
v	Virtual mass
w	Ocean wave
x	Horizontal direction
y	Vertical direction
ϕ	Angle of the cable with the vertical

Superscripts

$\cdot$	d/dt

ABSTRACT

A two-degree-of-freedom nonlinear model is presented for the two-dimensional dynamic motions of an extensible suspended cable system. The two degrees of freedom are the stretch and inclination of the cable. The dynamic and drag characteristics of the cable are carefully modeled. The equations of motion are derived by means of the Lagrange equations. The potential and kinetic energies of the cable are obtained by assuming that the cable stretches uniformly. In order to account for ocean wave particle velocities and current profiles which may vary with depth, the cable may be divided into an arbitrary number of segments to calculate normal and tangential drag. The phenomenon of cable slack is also modeled. A FORTRAN IV computer program, DM2DF, has been written. Numerical results from the program compare favorably with some experimental measurements.

ADMINISTRATIVE INFORMATION

This work was sponsored by the Naval Air Systems Command under Air Task 5335330/440C/1WZ1400000.

INTRODUCTION

Since the turn of the century, the study of the motion behavior of flexible cable systems has been an area of active interest. For a review of cable studies to date, see the excellent review article by Casarella and Parsons.[1]

The earlier investigations of the dynamic motions of cables usually restricted the motions to one direction only. In these studies, the cable was assumed to be a straight line and motions were either parallel or normal to the line. The equations studied were basically those for the longitudinal motions of an extensible rod or the lateral motions of a vibrating string. In recent years, with the development of high-speed electronic computers, cable dynamics studies have allowed the cable to have motions in two or all three directions. Two principal approaches have been used in studies of the full two-dimensional and three-dimensional nonlinear cable equations of motion.

One approach has been to directly solve the partial differential equations de-

[1] References are listed on page 34.

scribing the dynamic motions of the cable. This approach has been taken by Schram,[2] Huffman,[3] and Nath.[4] All three authors used some form of the method of characteristics to solve the dynamic cable equations. This method basically reduces the solution of the original set of partial differential equations to integrating a set of ordinary differential equations along certain characteristics directions, which may be obtained with relative ease. This method may be used for hyperbolic systems of partial differential equations. The dynamic cable equations form a set of first-order hyperbolic partial differential equations if internal damping is neglected and the cable is taken to be extensible.

Huffman considered the two-dimensional dynamic motions of an extensible cable towed from an airplane. Nath considered the two-dimensional dynamic motions of an estensible cable moored in water. Both Huffman and Nath allowed for internal damping. Huffman points out that for small amounts of internal damping, the hyperbolic character of the system is preserved. Schram considered the three-dimensional dynamic motions of an inextensible cable towed from a ship. Since the cable is inextensible, some of the equations in the Schram formulation are not hyperbolic. Since the method of characteristics is not applicable for these equations, Schram used another scheme for their solution.

The alternate approach has been to consider the cable as being composed of a number of straight segments. For each segment, a set of differential equations is written. By using this approach, the problem of solving several partial differential equations is changed to the problem of solving a large number of ordinary differential equations. This approach has been used by Strandhagen and Thomas,[5] Walton and Polachek,[6] Polachek et al.,[7] the Boeing Company (as reported by Schram[2]), and Froidevaux and Scholten.[8] Strandhagen and Thomas formulated the three-dimensional equations of motion of an inextensible cable divided into a number of rigid segments connected by universal joints. They did not give methods of solution. According to Schram, the Boeing Company extended this formulation to allow moments to be transmitted between segments and used an analog computer to obtain the solution. The remaining studies all considered two-dimensional motions. Froidevaux and Scholten used the Runge-Kutta method to directly solve the differential equations on a digital

computer. Walton and Polachek[6] and Polachek et al.[7] converted the differential equations into a number of finite difference equations and used matrix methods to solve the resulting set of algebraic equations. In References 6-8, it is pointed out that for inextensible cables the solutions must be iterated a number of times in order to ensure that the cable is geometrically continuous. For extensible cables, no such iterations are required, but the time steps which advance the solution forward in time must be very small in order for the numerical scheme to be stable.

Computer time requirements, in all cases where they have been reported in the above studies, have been quite large. Schram[2] reports that about one hour of digital computer time, using an IBM 7044, is required to obtain four seconds of cable motion. Froidevaux and Scholten[8] report that, for the elastic cable, about 100 seconds of computer time are required for one second of cable motion. According to Reference 9, Walton, in a private communication, estimated that it would take 20 hours of IBM 7090 time to calculate one case. It may be noted that in References 6 and 7 one case consists of about 50 seconds of cable motion. In terms of cost, this means that each case would cost hundreds of dollars.

In view of the large computer time requirements in the above studies, some recent studies have investigated approximate solutions to the nonlinear cable partial differential equations of motion. Paquette and Henderson[9] and Kerney[10] have considered the dynamic motions to be perturbations about the steady-state configuration. The result is to simplify the dynamic cable equations. In both studies, the motions are taken to be two-dimensional. Paquette and Henderson considered the cable to be segmented and expressed the differential equations in terms of finite difference equations, similar to the approach used in References 6 and 7. By assuming the dynamic motions to be small, their resulting set of finite difference equations is linear and much simpler than those in References 6 and 7. They programmed their formulation for solution on an analog computer and report that each case took about 10 minutes. Kerney directly linearized the partial differential equations by considering the dynamic motions to be small. Neglecting transient motions, the response of the linear system to a sinusoidal disturbance with frequency f is also a sinusoidal function with the same frequency. In this case, derivatives with respect to time may be re-

placed by $i\omega$ where $i = \sqrt{-1}$ and $\omega = 2\pi f$. The linear partial differential equations reduce to a set of ordinary differential equations with the distance along the cable s as the only independent variable. Kerney has programmed his formulation for solution on digital computers.

Paul and Soler[11] have considered the dynamic motions of a cable towed by a surface ship which undergoes discrete changes in its towing velocity. Paul and Soler show that in this case inertia terms may be neglected. As a result, the differential equations describing the motions of a segmented cable contain only first-order derivatives, resulting in a considerable simplification of the problem. They report that it takes only one second of IBM 360 time to compute 87 seconds of cable motion.

The present report also presents an approximate analysis of the two-dimensional dynamic motions of a cable which is either towed or free-floating. The cable is restricted to two degrees of freedom. The cable is allowed to stretch like a spring and swing like a pendulum. The present study is an extension of a study by Chey,[12] who has considered a somewhat similar model. The present study pays considerably more attention to the dynamic and drag characteristics of the cable. Also, Chey restricts the cable to small angular motion and programs his formulation for solution on an analog computer. In the present study, the angular motions may be large and the formulation is programmed for solution on digital computers.

The equations of motion are presented in the form of Lagrange equations. The two generalized coordinates are the angular swing and stretch of the cable. By using Lagrangian methods, most of the terms in the equations of motion are obtained by taking appropriate derivatives of the kinetic and potential energies of the cable system. The potential and kinetic energies of the cable are derived by assuming that the cable stretches uniformly. It is pointed out that this approach leads to first approximations for the fundamental natural frequencies of the cable system. Fluid drag forces, which are dissipative, are considered separately. In calculating the cable drag forces, the cable may be divided into an arbitrary number of segments. This gives an accurate description of the drag forces acting on the cable in the presence of a current profile which varies with depth. A Voigt model is used for cable internal damping, where the damping is proportional to rate of strain. The cable thickness is assumed to change linearly with the strain.

A description is given of the FORTRAN IV computer program based on the above analysis. The program allows for periodic motions which are represented by an arbitrary number of sinusoidal motions in the horizontal and/or vertical directions at the top of the cable. With very minor changes in program logic, nonperiodic motions may also be prescribed at the top of the cable. A current profile varying with depth may also be read in. Water particle velocities due to ocean waves are also considered. Cable parameters such as spring coefficient AE, where A is the area of a cross section of the cable and E is the modulus of elasticity, length, and thickness are read in corresponding to a reference value of the tension. The use of the reference tension is important for cases where the cable is highly extensible (i.e., undergoes large changes in cable dimensions for relatively small changes in tension) and/or has a spring coefficient which changes with tension. In these cases, the reading in of reference cable parameters corresponding to the steady-state tension will serve to accurately describe dynamic motions about the steady-state shape. The user may, by reading in the appropriate value for a given input variable, prescribe that tensions in the cable are always greater than or equal to a given value. It should be noted that for most cases of flexible cables, the cable cannot support a compressive force, i.e., the tension must be greater or equal to zero.

The various numerical checks which have been made on the correctness of the program are described. It is shown that the results from the present analysis are in fairly good agreement with some experimental results obtained by Dale et al.[13] The importance of validating the present model is pointed out. The report concludes by discussing some possible extensions of the present model.

DERIVATION OF EQUATIONS

The dynamic model considered in the present study is given in Figure 1. The two degrees of freedom, or generalized coordinates, are the stretch u of the bottom of the cable and the angle ϕ which the cable makes with the vertical. With the choice of coordinates used in the present study, with the x-axis positive to the right and the y-axis positive downwards, ϕ is positive in a clockwise direction.

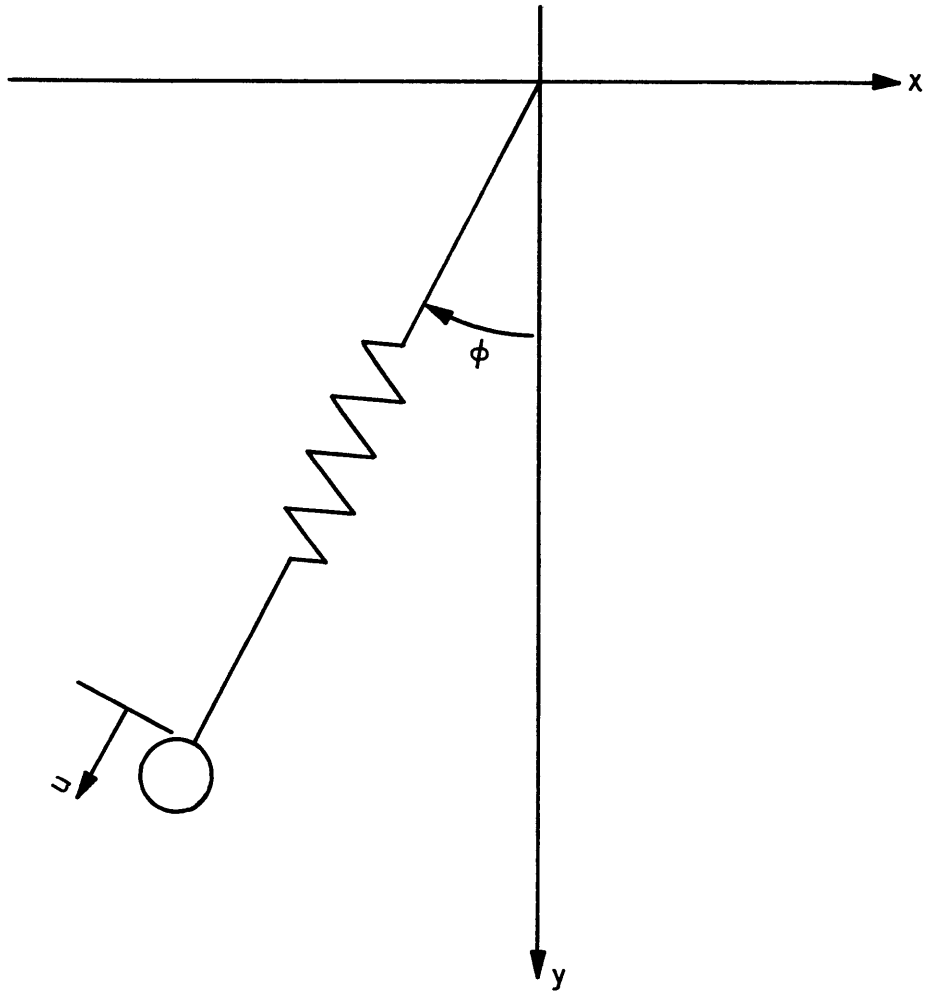

Figure 1 - Two-Degree-of-Freedom Dynamic Model

RELATIONSHIPS BETWEEN CABLE PARAMETERS AT DIFFERENT TENSIONS

In the following derivation, cable parameters such as length, thickness, and mass per unit length are expressed, for convenience, in terms of these quantities at zero tension. Cable quantities at zero tension are written with a subscript "o." Cable quantities are read in, however, for a reference tension which need not be equal to zero. Cable parameters for the reference tension are denoted with a subscript "r." The importance of reading in cable data for the reference tension equal to the steady-state tension in cases of highly extensible cables and/or cables with variable spring coefficients AE has been pointed out in the Introduction. In these cases, the cable parameters for zero tension, derived below, may be substantially different from the true values of the cable parameters at zero tension. The "zero tension" cable parameters for these cases should be simply regarded as fictitious quantities which facilitate the analysis given in later sections.

The cable length at zero tension ℓ_o is simply related to the reference cable length ℓ_r by

$$\ell_o = \ell_r - \frac{T_r}{k} \qquad (1)$$

where T_r is the reference tension,

k is the spring constant $= (AE)_r/\ell_r$, and

$(AE)_r$ is the reference spring coefficient.

In the above equation it may be noted that the spring constant is referred to the reference length ℓ_r . Similarly, the strain e is defined by

$$e = \frac{u}{\ell_r} \qquad (2)$$

where $u = \ell - \ell_o$.

In the present study, the cable thickness d is assumed to change linearly with the strain as follows

$$d = d_0 (1 - p\frac{u}{\ell_r}) \tag{3}$$

The above equation simply gives the contraction in the lateral direction of an elastic material undergoing a strain u/ℓ_r in the longitudinal direction. The cable thickness d_0 for zero tension is then simply related to the reference cable thickness d_r by

$$d_0 = d_r / \left(1 - p\,\frac{T_r}{k\ell_r}\right) \tag{4}$$

It should be noted that for the case of round cables the quantity d is simply the cable diameter.

The relationship between cable mass per unit length at an arbitrary tension, m, and cable mass per unit length at zero tension, m_0, may be obtained by noting that the total cable mass does not change as the cable stretches. Assuming that the cable stretches uniformly, the following equations hold

$$m(\ell_0 + u) = m_0 \ell_0 = m_r \ell_r \tag{5}$$

$$m = \frac{m_0 \ell_0}{\ell_0 + u} \tag{6a}$$

$$m_0 = \frac{m(\ell_0 + u)}{\ell_0} = \frac{m_r \ell_r}{\ell_0} \tag{6b}$$

From Equation (6b), m_0 in terms of m_r is given by

$$m_0 = \frac{m_r \ell_r}{\ell_0} \tag{7}$$

LAGRANGE EQUATIONS

The equations of motion are derived in the form of Lagrange equations. For the two generalized coordinates u and ϕ, the Lagrange equations take the form

$$\frac{d}{dt}\left(\frac{\partial L}{\partial \dot{u}}\right) - \frac{\partial L}{\partial u} = Q_{cu} + Q_{bu} + Q_{Iu} \tag{8}$$

$$\frac{d}{dt}\left(\frac{\partial L}{\partial \dot{\phi}}\right) - \frac{\partial L}{\partial \phi} = Q_{c\phi} + Q_{b\phi} \tag{9}$$

where t is the time,

$\cdot$ denotes differentiation with respect to time,

L is the Lagrangian $= K - V$,

K is the kinetic energy of the cable system,

V is the potential energy of the cable system,

Q_{cu} is the tangential drag acting on the cable,

Q_{bu} is the component of drag acting on the lower body parallel to the cable,

Q_{Iu} is the cable internal damping,

$Q_{c\phi}$ is the moment about the top of the cable due to the normal drag acting on the cable, and

$Q_{b\phi}$ is the moment about the top of the cable due to the component of drag acting on the lower body normal to the cable.

It should be noted that the terms on the right side of Equations (8) and (9) refer to moments and forces which arise due to fluid viscosity and cable structural damping, and hence, are not derivable from the Lagrangian L. Also, the terms on the right side of Equation (9) are moments, which are the "generalized forces" corresponding to the generalized angle ϕ.

For the purpose of calculating the potential and kinetic energies, it is useful to note the following geometrical relationships:

$$x_c = x_s - (1/2)(\ell_o + u)\sin\phi \tag{10a}$$

$$x_b = x_s - (\ell_o + u)\sin\phi \tag{10b}$$

$$y_c = y_s + (1/2)(\ell_o + u)\cos\phi \tag{10c}$$

$$y_b = y_s + (\ell_o + u)\cos\phi \tag{10d}$$

$$\dot{x}_b = \dot{x}_s - \dot{u}\sin\phi - (\ell_o + u)\cos\phi\dot{\phi} \tag{11a}$$

$$\dot{y}_b = \dot{y}_s + \dot{u}\cos\phi - (\ell_o + u)\sin\phi\dot{\phi} \tag{11b}$$

where x_c, y_c refer to the x and y displacements of the midpoint of the cable,

x_b, y_b refer to the x and y displacements of the lower body, and

x_s, y_s refer to the prescribed x and y displacements of the top of the cable.

Potential Energy

The potential energy of the system is due to the gravity potential of cable and body and the strain energy due to cable stretch. The gravity potentials are simply due to the change in height of the centers of mass of the body and cable. For the uniform cable considered in the present study, the cable center of mass is simply located at the midpoint of the cable. The gravity potential V_g is then given by

$$\begin{aligned} V_g &= -W_b y_b - W_c y_c \\ &= -W_b\left[y_s + (\ell_o + u)\cos\phi\right] - W_c\left[y_s + \tfrac{1}{2}(\ell_o + u)\cos\phi\right] \end{aligned} \tag{12}$$

where W_b is the weight in water of the body, and W_c is the weight in water of the cable.

Strictly speaking, the weight in water of the cable changes as the cable stretches due to a possible change in the volume displaced by the cable. In view of the approximate nature of the present study, W_c is regarded as a constant.

The strain energy V_e for the longitudinal vibrations of a uniform elastic spring of length ℓ_r and spring coefficient $(AE)_r$ is given by[13]

$$V_e = \frac{1}{2}(AE)_r \int_0^{\ell_r} \left(\frac{\partial w}{\partial s}\right)^2 ds \tag{13}$$

where s is distance measured along the spring, and w is the stretch of the spring at point s.

In the case when the spring has mass, a partial differential equation must be solved in order to obtain the proper values of w to substitute into Equation (13).[14] Timoshenko and Young[15] point out that as a first approximation, the displacements of a spring with mass may be considered to be the same as those for a spring without mass. It may be noted that in this case the spring stretches uniformly. Using this approximation, the strain energy for a spring with mass is equal to the strain energy of a massless spring, which is given in standard textbooks on vibrations as

$$V_e = \frac{1}{2}ku^2 \tag{14}$$

The total potential energy of the system is then given by the sum of Equations (12) and (14)

$$\begin{aligned} V &= V_g + V_e \\ &= -W_b\left[y_s + (\ell_0+u)\cos\phi\right] - W_c\left[y_s + \frac{1}{2}(\ell_0+u)\cos\phi\right] + \frac{1}{2}ku^2 \end{aligned} \tag{15}$$

Kinetic Energy

The kinetic energy of the system is the sum of the kinetic energies of the lower body and the cable.

Assuming no rotation, the kinetic energy K_b of the lower body is simply given by

Lower Body

$$K_b = \frac{1}{2}(M_{bvx}\,\dot{x}_b^2 + M_{bvy}\,\dot{y}_b^2)$$
$$= \frac{1}{2}\left\{M_{bvx}\left[\dot{x}_s - \dot{u}\sin\phi - (\ell_o + u)\cos\phi\dot{\phi}\right]^2\right. \tag{16}$$
$$\left. + M_{bvy}\left[\dot{y}_s + \dot{u}\cos\phi - (\ell_o + u)\sin\phi\dot{\phi}\right]^2\right\}$$

where M_{bvx} is the virtual mass, the mass plus added mass, of the body for motion in the x direction, and M_{bvy} is the virtual mass of the body for motion in the y direction.

The kinetic energy due to cable motion may be divided into two parts: kinetic energy due to motion of the cable parallel to itself, and kinetic energy due to motion normal to itself. To obtain the kinetic energies, it is necessary to compute the normal and tangential velocities of the cable. The normal and tangential components of the prescribed velocities at the top of the cable system, v_{sn} and v_{st}, respectively, are given by

Cable

$$v_{sn} = -\dot{y}_s\sin\phi - \dot{x}_s\cos\phi \tag{17a}$$

$$v_{st} = \dot{y}_s\cos\phi - \dot{x}_s\sin\phi \tag{17b}$$

At a distance s from the top of the cable, the normal velocity of the cable due to cable swing, v_{pn}, is simply given by

Normal

$$v_{pn} = s\dot{\phi} \tag{18}$$

To obtain the longitudinal velocity $\dot{w}$ for a spring with mass, one must, as previously pointed out, solve a partial differential equation.[14] As a first approximation, Timoshenko and Young[15] point out that $\dot{w}$ may be assumed to be a linear function of s, as follows

Tang.

$$\dot{w} = \frac{s\dot{u}}{(\ell_o + u)} \tag{19}$$

where $\dot{u}$ is the stretch velocity of the cable at the lower body.

The tangential and normal velocities of the cable at a point s, v_{ct} and v_{cn}, respectively, are then given by

$$v_{ct} = v_{st} + \dot{w} = \dot{y}_s \cos\phi - \dot{x}_s \sin\phi + \frac{s\dot{u}}{\ell_o + u} \tag{20a}$$

$$v_{cn} = v_{sn} + v_{pn} = -\dot{y}_s \sin\phi - \dot{x}_s \cos\phi + s\dot{\phi} \tag{20b}$$

The kinetic energy dK_{ct} due to tangential motion of a cable segment of length ds is given by

$$dK_{ct} = \frac{1}{2} \frac{m_o \ell_o}{\ell_o + u} ds \left[\dot{y}_s \cos\phi - \dot{x}_s \sin\phi + \frac{s\dot{u}}{\ell_o + u}\right]^2 \tag{21}$$

In the above expression, use has been made of the mass relationship given by Equation (6a). The kinetic energy K_{ct} due to tangential velocity of the entire cable is given by integrating Equation (21) with respect to s, from s = 0 to s = $\ell_o + u$, resulting in

$$K_{ct} = \frac{1}{2} m_o \ell_o \left[(-\dot{x}_s \sin\phi + \dot{y}_s \cos\phi)^2 + (-\dot{x}_s \sin\phi + \dot{y}_s \cos\phi)\dot{u} + \frac{\dot{u}^2}{3}\right] \tag{22}$$

The kinetic energy dK_{cn} due to normal velocity of a cable segment of length ds is given by

$$dK_{cn} = \frac{1}{2}\left[\frac{m_o \ell_o ds}{\ell_o + u} + \gamma \frac{\rho \pi d_o^2}{4}\left(1 - \frac{pu}{\ell_r}\right)^2 ds\right]\left[-\dot{y}_s \sin\phi - \dot{x}_s \cos\phi + s\dot{\phi}\right]^2 \tag{23}$$

where ρ is the fluid density, and γ is the added mass coefficient.
In the above equation, the second term within the first pair of brackets represents the added mass. For circular cables, γ is simply equal to 1. Integrating the above equation from s = 0 to s = $\ell_o + u$ yields the following expression for K_{cn}, the kinetic energy of the entire cable due to normal velocity

$$K_{cn}=\frac{1}{2}\left[m_o \ell_o+\frac{\gamma\rho\pi d_o^2}{4}\left(1-\frac{pu}{\ell_r}\right)^2(\ell_o+u)\right]\left[-\dot{y}_s \sin\phi-\dot{x}_s\cos\phi)^2\right. \tag{24}$$
$$\left.-(\dot{y}_s\sin\phi+\dot{x}_s\cos\phi)\dot{\phi}(\ell_o+u)+\frac{(\ell_o+u)^2\dot{\phi}^2}{3}\right]$$

It is of interest to note that the expressions for kinetic energy given in Equations (22) and (24) differ from the expressions which would result if the kinetic energies were based simply on the velocities at the center of mass of the cable, i.e., the time derivatives of x_c and y_c given in Equations (10a) and (10c). In this case, the term $\dot{u}^2/3$ in Equation (22) would be replaced by $\dot{u}^2/4$ and the term $(\ell_o+u)^2\dot{\phi}^2/3$ in Equation (24) would be replaced by $(\ell_o+u)^2\dot{\phi}^2/4$.

The total kinetic energy K is given by the sum of Equations (16), (22), and (24), resulting in

$$K=K_b+K_{ct}+K_{cn}=\frac{1}{2}M_{bvx}\left[\dot{x}_s-\dot{u}\sin\phi-(\ell_o+u)\cos\phi\dot{\phi}\right]^2$$
$$+\frac{1}{2}M_{bvy}\left[\dot{y}_s+\dot{u}\cos\phi-(\ell_o+u)\sin\phi\dot{\phi}\right]^2 \tag{25}$$
$$+\frac{1}{2}M_c\left[(-\dot{x}_s\sin\phi+\dot{y}_s\cos\phi)^2+(-\dot{x}_s\sin\phi+\dot{y}_s\cos\phi)\dot{u}+\frac{\dot{u}^2}{3}\right]$$
$$+\frac{1}{2}M_{cv}\left[(-\dot{y}_s\sin\phi-\dot{x}_s\cos\phi)^2-(\dot{y}_s\sin\phi+\dot{x}_s\cos\phi)\dot{\phi}(\ell_o+u)+\frac{(\ell_o+u)^2\dot{\phi}^2}{3}\right]$$

where $M_c=m_o\ell_o=m_r\ell_r$, and $M_{cv}=M_c+\frac{\gamma\rho\pi d_o^2}{4}\left(1-\frac{pu}{\ell_r}\right)^2(\ell_o+u)$.

DRAG FORCES

Fluid Velocities

Fluid drag forces arise from the difference between the fluid and cable system velocities. In the present study a current profile variable with depth and water particle velocities due to surface waves are considered.

For ocean depths greater than one-half the wave length, the water particle velocities due to surface waves are given by[16]

$$\dot{x}_w = ae^{-ny}\sigma \sin(nx-\sigma t) \tag{26a}$$

$$\dot{y}_w = ae^{-ny}(-\sigma)\cos(nx-\sigma t) \tag{26b}$$

where $\dot{x}_w$ is the water particle velocity in the x direction,

$\dot{y}_w$ is the water particle velocity in the y direction,

a is the wave amplitude,

$n = 2\pi/\lambda$, wave #

λ is the wave length,

$\sigma = \sqrt{2\pi g/\lambda}$, and

g is gravity constant = 32.2 ft/sec^2.

The ocean environmental velocities at point (x, y) are then given by

$$\dot{\xi}(x,y,t) = c(y) + \dot{x}_w \tag{27}$$

$$\dot{\eta}(x,y,t) = \dot{y}_w \tag{28}$$

where $\dot{\xi}$ is the ocean velocity in the x direction,

$\dot{\eta}$ is the ocean velocity in the y direction, and

c(y) is the steady horizontal fluid flow relative to the cable system and is composed of the actual current profile, which may be a function of depth, minus the steady-state speed of the cable system.

In the present study, the cable is divided into N equal segments for the purposes of calculating the viscous fluid forces, where the number N is read into the program. Thus, in order to compute the viscous forces acting on the cable system, it is necessary to evaluate $\dot{\xi}$ and $\dot{\eta}$ at the lower body and at the midpoints of the N cable segments. The values of $\dot{\xi}$ and $\dot{\eta}$ at the lower body, denoted by $\dot{\xi}_b$ and $\dot{\eta}_b$, respectively, are given by

$$\dot{\xi}_b = \dot{\xi}(x_b, y_b, t) \tag{29a}$$

$$\dot{\eta}_b = \dot{\eta}(x_b, y_b, t) \tag{29b}$$

where x_b and y_b are given in Equations (10b) and (10d), respectively.

The values of x_{ci} and y_{ci}, the values of x and y at the midpoint of the i^{th} cable segment, where i = 1 corresponds to the topmost cable segment, are given by

$$x_{ci} = x_s - \left[\left(i - \frac{1}{2}\right)\frac{\ell_o + u}{N}\right]\sin\phi \tag{30a}$$

$$y_{ci} = y_s + \left[\left(i - \frac{1}{2}\right)\frac{\ell_o + u}{N}\right]\cos\phi \tag{30b}$$

The values of $\dot{\xi}_{ci}$ and $\dot{\eta}_{ci}$, the values of $\dot{\xi}$ and $\dot{\eta}$ at the midpoint of the ith segment, are given by

$$\dot{\xi}_{ci} = \dot{\xi}(x_{ci}, y_{ci}, t) \tag{31a}$$

$$\dot{\eta}_{ci} = \dot{\eta}(x_{ci}, y_{ci}, t) \tag{31b}$$

where x_{ci} and y_{ci} are defined above.

Drag Forces on the Lower Body

Consider now the drag forces acting on the lower body. In the present report, the term drag refers to those forces which are proportional to the square of the relative fluid velocity. In general, the drag forces acting on a body vary in a complex manner

with the direction of the flow relative to the body. Except for standard shapes such as spheres, circular cylinders, and thin discs, this variation is not well known. Due to the complete symmetry of the sphere, the resultant drag force always acts in the same direction as the relative fluid velocity. It may be noted that for two-dimensional motions the preceding remark also applies to the case of a circular cylinder with its longitudinal axis perpendicular to the plane of motion. In general, the resultant drag force will not be in the same direction as the relative flow. For example, for thin disks and long circular cylinders with axes in the plane of motion, the drag forces are usually written in terms of two parts: a drag normal to the cylinder axis or disk face, proportional to the square of the normal velocity, and a drag tangential to the cylinder axis or disk face, proportional to the square of the tangential velocity.[17] Usually, the normal drag is much higher than the tangential drag. As is shown later in Equations (42) and (44), this is how the drag forces on the cable have been calculated.

The preceding discussion shows that even for the case of the three standard shapes, no single expression for drag is applicable to all three shapes. For example, Paul and Soler[11] use two expressions for the drag acting on the lower body, one appropriate for spheres and the other appropriate for circular cylinders with their axes in the plane of motion. Expressions for the variation of the resultant drag with flow direction for an arbitrary general body must be written on a case by case basis. For most bodies, this variation would have to be determined experimentally. Drag data in most cases are presented only for flow along a few directions relative to the body.[17] Usually, these directions correspond to axes of symmetry for the body. In the present report, similar to the approach taken by Paul and Soler, two types of expressions are written for the drag forces acting on the lower body. The expressions are basically respectively appropriate for spheres, and cylinders or disks. It is shown below that the expression appropriate for spheres may also be approximately correct for certain cases of blunt symmetrical bodies.

For the case of spheres, the drag force D_b acts in the same direction as the flow,

with magnitude given by

$$D_b = \frac{1}{2}\rho C_D A_b v_b^2 \tag{32a}$$

where $C_D A_b$ is the drag area, and

$$v_b^2 = (-\dot{x}_b + \dot{\xi}_b)^2 + (-\dot{y}_b + \dot{\eta}_b)^2 \tag{32b}$$

The components of D_b in the x and y directions, denoted by D_{bx} and D_{by}, respectively, are then simply given by

$$D_{bx} = \frac{D_b(-\dot{x}_b + \dot{\xi}_b)}{v_b} = \frac{1}{2}\rho C_D A_b v_b (-\dot{x}_b + \dot{\xi}_b) \tag{32c}$$

$$D_{by} = \frac{D_b(-\dot{y}_b + \dot{\eta}_b)}{v_b} = \frac{1}{2}\rho C_D A_b v_b (-\dot{y}_b + \dot{\eta}_b) \tag{32d}$$

It has been previously mentioned that the resultant drag force is not, in general, parallel to the flow. The drag force is parallel to the flow when the flow direction coincides with an axis of symmetry of the body. Thus, as pointed out above, the drag force is always parallel to the flow for the case of a sphere. It is also likely that the resultant drag force will be nearly parallel to the flow for a body with a number of axes of symmetry. The results of Reference 17 also suggest that for certain blunt bodies, the drag areas for different flow directions are approximately the same. For example, for the case of a cube, the drag areas for flow perpendicular and at 45 degrees to a face differ from each other by less than 10 percent. Similarly, for the case of a short circular cylinder with length equal to diameter, the drag areas for flow perpendicular and parallel to the end faces again differ from each other by less than 10 percent. Thus, the above equations may yield approximate engineering results not only for spheres but also for certain cases of blunt symmetrical bodies.

For the case of thin disks and circular cylinders, it is appropriate to express the drag in terms of the normal and tangential drag, D_{bn} and D_{bt}, respectively, as follows

$$D_{bn} = \frac{1}{2}\rho(C_D A_b)_n \; v_{bn} \left|v_{bn}\right| \tag{33a}$$

$$D_{bt} = \frac{1}{2}\rho(C_D A_b)_t \; v_{bt} \left|v_{bt}\right| \tag{33b}$$

where $(C_D A_b)_n$ is the normal drag area, and $(C_D A_b)_t$ is the tangential drag area. Following the relationships given in Equations (17a) and (17b), v_{bn} and v_{bt}, the normal and tangential velocities, respectively, are given by

$$v_{bt} = -(-\dot{x}_b + \dot{\xi}_b)\sin\phi_b + (-\dot{y}_b + \dot{\eta}_b)\cos\phi_b \tag{34a}$$

$$v_{bn} = -(-\dot{x}_b + \dot{\xi}_b)\cos\phi_b - (-\dot{y}_b + \dot{\eta}_b)\sin\phi_b \tag{34b}$$

where ϕ_b is the angle of the tangential axis of the body with the y axis. For the case of a circular cylinder, the tangential axis is simply the longitudinal axis of the cylinder, while for a disk, it is defined as the intersection of the x-y plane with the plane of the disk. The sign convention for ϕ_b is the same as that for ϕ, shown in Figure 1. Since the present study does not take rotation of the body into account, the angle ϕ_b is taken to be the angle of the tangential axis of the body with the y axis under steady-state conditions. It is an input into the computer program. D_{bx} and D_{by} may be obtained from D_{bn} and D_{bt} by basically inverting the relations given in Equations (34a) and (34b) resulting in

$$D_{bx} = -\sin\phi_b \; D_{bt} - \cos\phi_b \; D_{bn} \tag{35a}$$

$$D_{by} = +\cos\phi_b \; D_{bt} - \sin\phi_b \; D_{bn} \tag{35b}$$

The two preceding approaches for the drag will yield reasonable approximations for many bodies of engineering interest. It must be emphasized that other forms for the drag can be conveniently incorporated into the program.

The components of drag of the lower body in the directions parallel and normal to the cable, denoted by D_{bt} and D_{bn}, respectively, are given by

$$D_{bt} = -D_{bx} \sin\phi + D_{by} \cos\phi \tag{36a}$$

$$D_{bn} = -D_{bx} \cos\phi - D_{by} \sin\phi \tag{36b}$$

The generalized forces Q_{bu} and $Q_{b\phi}$ due to lower body drag are given by

$$Q_{bu} = D_{bt} = -D_{bx} \sin\phi + D_{by} \cos\phi \tag{37a}$$

$$Q_{b\phi} = (\ell_o + u) D_{bn} = (\ell_o + u)(-D_{bx} \cos\phi - D_{by} \sin\phi) \tag{37b}$$

Drag Forces on the Cable

In order to compute the drag acting on the cable, it is necessary to know the cable velocities at the midpoints of the N cable segments. This is done by taking the time derivatives of x_{ci} and y_{ci} given in Equations (30a) and (30b), resulting in

$$\dot{x}_{ci} = \dot{x}_s - \left[\left(i - \frac{1}{2}\right)\frac{\ell_o + u}{N}\right]\cos\phi\dot{\phi} - \left(i - \frac{1}{2}\right)\frac{\dot{u}}{N}\sin\phi \tag{38a}$$

$$\dot{y}_{ci} = \dot{y}_s - \left[\left(i - \frac{1}{2}\right)\frac{\ell_o + u}{N}\right]\sin\phi\dot{\phi} + \left(i - \frac{1}{2}\right)\frac{\dot{u}}{N}\cos\phi \tag{38b}$$

It is more convenient to express the cable velocities in terms of components parallel and normal to the ith cable segment, denoted by v_{cti} and v_{cni}, respectively. Using relationships analogous to those given in Equations (36a) and (36b), and the expressions for $\dot{x}_{ci}$ and $\dot{y}_{ci}$ given above, v_{cti} and v_{cni} are given by

$$v_{cti} = -\dot{x}_s \sin\phi + \dot{y}_s \cos\phi + \left(i - \frac{1}{2}\right)\frac{\dot{u}}{N} \tag{39a}$$

$$v_{cni} = -\dot{x}_s \cos\phi - \dot{y}_s \sin\phi + \left(i - \frac{1}{2}\right)\frac{\ell_o + u}{N}\dot{\phi} \tag{39b}$$

Similarly, the components of fluid velocity parallel and normal to the ith cable segment, denoted by v_{fti} and v_{fni}, respectively, are given by

$$v_{fti} = -\dot{\xi}_{ci} \sin \phi + \dot{\eta}_{ci} \cos \phi \tag{40a}$$

$$v_{fni} = -\dot{\xi}_{ci} \cos \phi - \dot{\eta}_{ci} \sin \phi \tag{40b}$$

The normal and tangential velocities relative to the ith cable segment, v_{qni} and v_{qti}, respectively, are given by

$$v_{qni} = v_{fni} - v_{cni} \tag{41a}$$

$$v_{qti} = v_{fti} - v_{cti} \tag{41b}$$

Consider now the normal drag force acting on the cable. For bare cable the normal drag is usually written as being proportional to the square of the normal velocity relative to the cable. For the ith cable segment, the normal force D_{cni} takes the form

$$D_{cni} = \frac{1}{2} \rho C_D d_o \left(1 - \frac{pu}{\ell_r}\right) \frac{\ell_o + u}{N} |v_{qni}| v_{qni} \tag{42}$$

where C_D is the normal drag coefficient.

The drag moment $Q_{c\phi}$ about the top of the cable due to the drag forces acting on the entire cable is obtained by multiplying each value of D_{cni} by the moment arm $(\ell_o + u)(i - 1/2)/N$ and summing from $i = 1$ to $i = N$, resulting in

$$Q_{c\phi} = \frac{1}{2} \rho C_D d_o \left(1 - \frac{pu}{\ell_r}\right) \left(\frac{\ell_o + u}{N}\right)^2 \sum_{i=1}^{N} \left(i - \frac{1}{2}\right) |v_{qni}| v_{qni} \tag{43}$$

There is considerable variation among the forms proposed by different authors for the tangential drag acting on bare cable. In the present study the tangential drag is taken to be proportional to the square of the velocity tangential to the cable. This form has been used by Reber,[18] Richtmyer,[19] Wilson,[20] and Schneider and Nickels.[21] For the ith cable segment, the tangential drag D_{cti} takes the form

$$D_{cti} = \frac{C_t}{2} \rho d_o \underbrace{\left(1 - \frac{pu}{\ell_r}\right)\left(\frac{\ell_o + u}{N}\right)}_{\alpha} |v_{qti}| v_{qti} \tag{44}$$

where C_t is an experimentally measured friction coefficient. Other forms can, of course, be conveniently incorporated into the analysis.

The tangential drag force Q_{cu} due to the tangential forces acting on the entire cable is obtained by summing D_{cti} from i = 1 to i = N

$$Q_{cu} = \frac{C_t}{2} \rho d_o \left(1 - \frac{pu}{\ell_r}\right)\left(\frac{\ell_o + u}{N}\right) \sum_{i=1}^{N} |v_{qti}| v_{qti} \tag{45}$$

INTERNAL DAMPING

Under cyclic loading and unloading, most cables exhibit hysteresis loops; see, for example, Reid.[22] The existence of these loops implies that the stored strain energy is not entirely elastic and that there are energy losses due to internal structural damping. A number of models have been proposed for describing the internal damping. A rather complex model, involving several equations, has been proposed by Reid. In the present study, the internal damping Q_{Iu} is assumed to be proportional to the rate of strain, as follows

$$Q_{Iu} = -\frac{C_I}{\ell_r} \frac{du}{dt} \tag{46}$$

where C_I is the damping constant.

The above model for internal damping is commonly referred to as the Voigt model and has been used by Huffman[3] and Goeller and Laura.[23] Goeller and Laura experimentally show that the Voigt model adequately describes internal damping for nylon ropes except for frequencies of cable motion significantly higher than the resonance

frequency. Due to the nonlinear nature of the analysis considered in the present study, other forms of internal damping can be conveniently incorporated.

FINAL EQUATIONS

Equations (37a), (37b), (43), (45), and (46) define the right sides of Equations (8) and (9). It now remains to perform the various differentiations shown on the left sides of Equations (8) and (9). The Lagrangian L, upon which the various derivatives are performed, is simply the kinetic energy K, given in Equation (25), minus the potential energy V, given in Equation (15). Upon performing the various differentiations, and solving the resulting two equations for $\ddot{\phi}$ and $\ddot{u}$, the following two differential equations are obtained

$$\ddot{\phi} = \frac{A_3 R_1 - A_2 R_2}{A_1 A_3 - A_2^2} \tag{47}$$

$$\ddot{u} = \frac{A_1 R_2 - A_2 R_1}{A_1 A_3 - A_2^2} \tag{48}$$

where $A_1 = (\ell_0+u)^2\left(\frac{M_{cv}}{3} + M_{bvx}\cos^2\phi + M_{bvy}\sin^2\phi\right)$

$A_2 = (\ell_0+u)\sin\phi\cos\phi\,(M_{bvx} - M_{bvy})$

$A_3 = \frac{M_c}{3} + M_{bvx}\sin^2\phi + M_{bvy}\cos^2\phi$

$R_1 = -S_H - S_A - S_B - S_C + S_D + S_E + S_F + S_G - \frac{dV}{d\phi} + Q_{b\phi} + Q_{c\phi}$

$$S_H = 0.5\rho\gamma\frac{\pi d_o^2}{4}\left[\dot{u}\left(1-\frac{pu}{\ell_r}\right)^2 + 2(\ell_0+u)\left(1-\frac{pu}{\ell_r}\right)\left(-\frac{p\dot{u}}{\ell_r}\right)\right]\cdot \left[(-\dot{y}_s\sin\phi - \dot{x}_s\cos\phi)(\ell_0+u) + \frac{2}{3}(\ell_0+u)^2\dot{\phi}\right]$$

$$S_A = \frac{M_{cv}}{2}\left[(-\ddot{y}_s\sin\phi - \dot{y}_s\cos\phi\dot{\phi} - \ddot{x}_s\cos\phi + \dot{x}_s\sin\phi\dot{\phi})(\ell_0+u) + (-\dot{y}_s\sin\phi - \dot{x}_s\cos\phi)\dot{u} + \frac{4(\ell_0+u)\dot{u}\dot{\phi}}{3}\right]$$

$$S_B = M_{bvx}\{[\ddot{x}_s - \dot{u}\cos\phi\dot{\phi} + (\ell_o+u)\sin\phi\dot{\phi}^2 - \dot{u}\cos\phi\dot{\phi}][-(\ell_o+u)\cos\phi]$$
$$+[\dot{x}_s - (\ell_o+u)\cos\phi\dot{\phi} - \dot{u}\sin\phi][-\dot{u}\cos\phi + (\ell_o+u)\sin\phi\dot{\phi}]\}$$

$$S_C = M_{bvy}\{[\ddot{y}_s - \dot{u}\sin\phi\dot{\phi} - (\ell_o+u)\cos\phi\dot{\phi}^2 - \dot{u}\sin\phi\dot{\phi}][-(\ell_o+u)\sin\phi]$$
$$+[\dot{y}_s - (\ell_o+u)\sin\phi\dot{\phi} + \dot{u}\cos\phi][-\dot{u}\sin\phi - (\ell_o+u)\cos\phi\dot{\phi}]\}$$

$$S_D = \frac{M_{cv}}{2}(-\dot{y}_s\cos\phi + \dot{x}_s\sin\phi)[2(-\dot{y}_s\sin\phi - \dot{x}_s\cos\phi) + (\ell_o+u)\dot{\phi}]$$

$$S_E = \frac{M_c}{2}(-\dot{x}_s\cos\phi - \dot{y}_s\sin\phi)[2(-\dot{x}_s\sin\phi + \dot{y}_s\cos\phi) + \dot{u}]$$

$$S_F = M_{bvx}[\dot{x}_s - (\ell_o+u)\cos\phi\dot{\phi} - \dot{u}\sin\phi][(\ell_o+u)\sin\phi\dot{\phi} - \dot{u}\cos\phi]$$

$$S_G = M_{bvy}[\dot{y}_s - (\ell_o+u)\sin\phi\dot{\phi} + \dot{u}\cos\phi][-(\ell_o+u)\cos\phi\dot{\phi} - \dot{u}\sin\phi]$$

$$\frac{dV}{d\phi} = (\ell_o+u)\sin\phi\left(\frac{W_c}{2} + W_b\right) \tag{49a}$$

$Q_{b\phi}$ is defined in Equation (37b).

$Q_{c\phi}$ is defined in Equation (43).

$$R_2 = -S_Z - S_Y - S_X + S_W - S_V - S_U + S_T - \frac{dV}{du} + Q_{bu} + Q_{cu} + Q_{Iu}$$

$$S_Z = \frac{M_c}{2}(-\ddot{x}_s\sin\phi - \dot{x}_s\cos\phi\dot{\phi} + \ddot{y}_s\cos\phi - \dot{y}_s\sin\phi\dot{\phi})$$

$$S_Y = M_{bvx}\{[\ddot{x}_s - \dot{u}\cos\phi\dot{\phi} + (\ell_o+u)\sin\phi\dot{\phi}^2 - \dot{u}\cos\phi\dot{\phi}](-\sin\phi)$$
$$+[\dot{x}_s - (\ell_o+u)\cos\phi\dot{\phi} - \dot{u}\sin\phi](-\cos\phi\dot{\phi})\}$$

$$S_X = M_{bvy}\{[\ddot{y}_s - \dot{u}\sin\phi\dot{\phi} - (\ell_o+u)\cos\phi\dot{\phi}^2 - \dot{u}\sin\phi\dot{\phi}]\cos\phi$$
$$+[\dot{y}_s - (\ell_o+u)\sin\phi\dot{\phi} + \dot{u}\cos\phi](-\sin\phi\dot{\phi})\}$$

$$S_W = \frac{M_{cv}}{2}\left[(-\dot{y}_s\sin\phi - \dot{x}_s\cos\phi)\dot{\phi} + \frac{2(\ell_o+u)}{3}\dot{\phi}^2\right]$$

$$S_V = M_{bvx}[\dot{x}_s - (\ell_o+u)\cos\phi\dot{\phi} - \dot{u}\sin\phi](\cos\phi\dot{\phi})$$

$$S_U = M_{bvy}[\dot{y}_s - (\ell_o+u)\sin\phi\dot{\phi} + \dot{u}\cos\phi](\sin\phi\dot{\phi})$$

$$S_T=\frac{1}{2}\rho\gamma\frac{\pi d_o^2}{4}\left(1-\frac{pu}{\ell_r}\right)\left[\left(1-\frac{pu}{\ell_r}\right)+(\ell_o+u)\,2\left(\frac{-p}{\ell_r}\right)\right]\cdot$$

$$\left[(-\dot{y}_s\sin\phi-\dot{x}_s\cos\phi)^2+(-\dot{y}_s\sin\phi-\dot{x}_s\cos\phi)\dot{\phi}(\ell_o+u)+\frac{(\ell_o+u)^2}{3}\dot{\phi}^2\right]$$

$$\frac{dV}{du}=ku-\cos\phi\left(\frac{W_c}{2}+W_b\right) \tag{49b}$$

Q_{bu} is defined in Equation (37a).

Q_{cu} is defined in Equation (45).

Q_{Iu} is defined in Equation (46).

For convenience in programming, the two second-order differential Equations (47) and (48) may be rewritten as four first-order differential equations, as follows:

$$\phi_1=\dot{\phi} \tag{50}$$

$$u_1=\dot{u} \tag{51}$$

$$\dot{\phi}_1=\frac{A_3R_1-A_2R_2}{A_1A_3-A_2^2} \tag{52}$$

$$\dot{u}_1=\frac{A_1R_2-A_2R_1}{A_1A_3-A_2^2} \tag{53}$$

where the right sides of Equations (52) and (53) are identical with the respective right sides of Equations (47) and (48) with the exception that $\dot{\phi}$ is replaced by ϕ_1, and $\dot{u}$ by u_1.

FORTRAN IV COMPUTER PROGRAM

DESCRIPTION OF PROGRAM

A FORTRAN IV computer program, DM2DF, has been written for the preceding formulation. The program consists of a main program and three subroutines. The main program reads in the prescribed surface motion, environmental and reference cable parameters, and initial conditions for u, ϕ, $\dot{u}$, and $\dot{\phi}$. It prints out the input parameters, converts the reference cable parameters to parameters for zero tension, calls the subrouting KUTMER to solve the differential equations, and prints out the following variables at specified time intervals: t, ϕ, $\dot{\phi}$, u, $\dot{u}$, x_b, $\dot{x}_b$, y_b, and $\dot{y}_b$.

The differential Equations (50)-(53) are defined in the subroutine DAUX. The subroutine DAUX is called by the subroutine KUTMER, which uses the Kutta-Merson method for solving systems of first-order differential equations, to solve the differential equations. The differential equations are integrated to an accuracy of 0.1 percent. In order to calculate the drag forces, the subroutine DAUX calls the subroutine CUR to obtain the proper values of the current. This is the same current subroutine used in the program FF2E,[24] which is a FORTRAN IV program for the steady-state motion behavior of free-floating cable systems. Basically, the subroutine CUR linearly interpolates the input current points. As pointed out previously, in the present study, the input current profile is the actual ocean current profile minus the steady-state speed of the cable system. In program FF2E, the input current profile is the actual ocean current profile. For the case of a cable towed by a surface ship, the steady-state speed of the cable system is simply the speed of the surface ship. For free-floating cable systems, the steady-state drift speed of the system is known only after a steady-state analysis of these systems. Thus, in the case of free-floating cable systems, a program such as FF2E should first be used to determine the system drift speed.

Several features of the program are worthy of mention. The motions at the top of the cable system are read in as the sum of an arbitrary number of sinusoidal functions in the x and/or y directions.

The force exerted by the cable on the lower body, F_{cb}, is given by the sum of the spring force - ku and the internal damping force Q_{Iu}, given in Equation (46), resulting in the following expression for F_{cb}

$$F_{cb} = -\left(ku + \frac{C_I}{\ell_r}\frac{du}{dt}\right) = -F_{bc} \tag{54}$$

where F_{bc} is the force exerted by the body on the cable. With the sign convention used for u in the present study, the quantity F_{bc} is positive if the cable is in tension. As Equation (54) stands, F_{bc} may become negative. However, a flexible cable cannot support a compressive force, i.e., F_{bc} cannot be negative. In this case, the user of the program should simply read in the value of the input variable TENS equal to 0. The input variable TENS defines the least algebraic tension which may be supported by the spring. Thus, if the program is used to study the motion behavior of a metallic rod, which may support large compressive forces, a large negative quantity should be read in for TENS.

For the convenience of users of the program, the input drag data for the two approaches for drag are entered into the program by using the same set of program variables. Where the drag forces are defined by Equations (33a) and (33b), the program variables CDABN and CDABT correspond respectively to $(C_D A_b)_n$ and $(C_D A_B)_t$. In this case, the program variable PHIBD corresponds to the angle ϕ_b in degrees. The variable PHIBD should be read in as a value between -180 and +180. When the drag forces are computed by using Equations (32a) to (32d), CDABN and CDABT should be read in equal to each other and correspond to $C_D A_b$. In this case, any number with an absolute value greater than 180 is read in for PHIBD. This serves to tell the program that the drag forces are to be computed by Equations (32a) to (32d).

In certain cases, the virtual mass of the cable may be very small compared to the virtual mass of the lower body. This may occur when the lower body is very heavy or is a damper device with large projected areas. In these cases, it is not necessary to calculate those terms involving cable mass and added mass, resulting in a saving of computer time. By reading in any negative number for the input variable CBMAS,

the program bypasses the terms involving the cable mass. Specifically, the terms S_A, S_H, S_D, S_E, S_Z, S_W, and S_T, defined immediately after Equation (48), are set equal to zero. For cases where it is desired to include the cable mass terms, the user simply reads in any quantity greater than zero for CBMAS.

The computer time requirements depend on such factors as duration of time over which the cable motions are desired, input frequencies, whether cable mass terms are calculated or not, and cable extensibility. For most cases of cable extensibility, input frequencies corresponding to typical sea states, and including cable mass terms, one minute of cable motion requires about three minutes of IBM 7090 time. On the CDC 6700 computer currently being used at NSRDC, compilation time is about 60 seconds and execution time for one minute of cable motion is approximately 20 seconds. Computer time requirements increase somewhat as cable extensibility decreases, i.e., as cable spring constant increases.

ACCURACY OF THE PROGRAM

Direct Checks for Simple Cases

The computer program has been checked against various simple cases, for which analytic solutions are available. In all cases, the computer results agree with theoretically predicted results to at least four significant figures.

One case checked has been the case where the spring is taken to be vertical, i.e., $\phi = 0$, and drag terms are omitted. For the case where the spring is taken to be massless, the program has been checked for prescribed vertical motions at the top of the spring, with and without linear damping. The particular case corresponding to zero linear damping and frequency of the prescribed motion equal to the natural frequency of the spring was checked. In this case, the computer results showed, as expected, that the motion of the lower body showed an unbounded growth with time. For example, after fifty cycles of motion, a 1-foot vertical displacement at the top of the cable had been magnified to 150 feet at the lower body. The program has also been checked for the free vibrations of the spring, where the spring need not be massless. For the case where the spring has mass, the observed period of motion agrees with a result given by Timoshenko and Young.[15]

Another case checked has been the case of free pendular motions of the spring. In this case, all the drag forces are taken equal to zero, the spring is made nearly inextensible, and the prescribed motions are set equal to zero. For relatively small angular motions, the observed periods of motion for the spring with and without mass agree with the results given by Tong[25] for simple and compound pendulums, respectively.

Comparison with Experimental Results

The results from the computer program have been compared with some experimental results obtained by Dale et al.[13] using the circulating water channel at Naval Ship Research and Development Center. In these experiments a circular motion was imparted to the top of the cable. These experiments were conducted for several sets of cable system parameters and several water speeds. However, numerical results are given only for one set of system parameters at zero water speed. These system parameters are shown in Table 1. Table 1 also shows the full-scale values of these parameters.

A certain amount of guessing was required in order to arrive at the input variables which were entered into the program. For example, the cable mass and weight in water were derived by assuming the cable to be made up partly of metal and partly of a neutrally buoyant plastic. For the 9-foot cable, the total weight in water and total mass were calculated to be 0.0036 pounds and 0.000171 slugs, respectively. It should be noted that the cable weight is only about 15 percent of the submerged weight of the lower body. The relatively small magnitude of the cable mass with respect to the lower body mass is also shown by a result in Reference 13 which shows that a calculated value for the natural frequency for the horizontal motions of the cable, in which cable mass is neglected, agrees to within 14 percent with the experimentally determined natural frequency for horizontal motions. Thus, moderate errors in cable weight and mass may not significantly affect the results. It was also uncertain what value to use for the spring coefficient AE. If half the area of the cable is assumed to be steel, AE is of the order of 1000 pounds. Computer runs were made for values of AE between 5 and 1000. It was found that to two significant

places, no differences were noted in the motions of the lower body. The reason for this was simply the fact that even in the case of AE = 5, the natural frequency for longitudinal motions of the cable was much higher than the frequencies of the prescribed motions. Since the cable is nearly inextensible, internal damping is not a significant factor here (since strain rates are small), and the internal damping coefficient was simply set equal to zero.

Table 2 compares the computed and measured amplitudes of motion of the lower body. On the whole, the results are encouraging. The agreement between the computer and experimental results is excellent for the vertical motions of the body. Both sets of results show that the vertical amplitude is flat and is equal to the amplitude of the prescribed motion. In the horizontal direction, the agreement is excellent for the lower frequencies. At the higher frequencies the computer results are in error by about 20 percent. Part of this error may be due to errors in the guessed input variables.

Discussion of Accuracy of the Present Model

While the preceding results are encouraging and constitute a partial validation of the model presented in the present study, more extensive comparisons with laboratory measurements, sea trial data, and/or more accurate models of cable motions must be made before the limits of validity of the present model can be clearly established. The following is a discussion of the probable accuracy of the present model.

In a sense, the present model may be considered as being a special case of the straight segment approach used in References 5-9. In particular, the present model may be viewed as representing the cable by one segment. It is felt that the present model yields more accurate results than a one-segment model using the approach taken in References 5-9. In these references, the cable dynamic and drag characteristics are taken to be lumped at the center of the segment. It has been pointed out that the cable dynamic characteristics, given in Equations (22) and (24), are not simply based on the velocities at the center of the cable. Also, the feature in the present model of dividing the cable into a number of segments for the purpose of calculating the drag enables the model to take into account a current profile varying with depth.

TABLE 1

Model and Full-Scale Parameters of Reference 13

	MODEL	FULL SCALE
Peak to peak amplitude of surface motion	5 inches	2.3 feet
Cable diameter (inches)	0.025	0.14
Cable length (feet)	9.0	50.0
Lower body shape	Sphere	Sphere
Lower body diameter (inches)	1.0	5.5
Lower body submerged weight (pounds)	0.025	4.18
System natural frequency ω_n (rad/sec)	1.14	0.49
System natural period (sec)	5.5	12.8
Current velocity (knots)	0.0	0.0

TABLE 2

Comparison of Computed and Measured Motions of the Lower Body

	$\frac{\omega}{\omega_n} = 0.5$	$\frac{\omega}{\omega_n} = 1.0$	$\frac{\omega}{\omega_n} = 1.5$	$\frac{\omega}{\omega_n} = 2.0$
x_{bA} (computed)	0.23	0.22	0.15	0.12
x_{bA} (measured)	0.23	0.21	0.12	0.10
y_{bA} (computed)	0.20	0.20	0.20	0.20
y_{bA} (measured)	0.21	0.21	0.21	0.21

Notes:

1. x_{bA}, y_{bA} are amplitudes of x_b and y_b in feet.
2. ω is forcing circular frequency in radians/sec.
3. ω_n is experimentally determined system natural frequency for horizontal motions in radians/sec.

The angle ϕ of the present model represents a value somewhere between the extremes of the values of ϕ along the actual cable at a given time. Thus, where the actual cable experiences only small angle changes along its scope (i.e., when the cable is nearly straight) such as in the case of relatively short cables and/or cables under large tension, the present model may yield accurate results. It should be noted that since the present analysis is nonlinear, the motions need not be small, as in the case of the linearized analyses of References 9 and 10. As cable scope increases, with accompanying larger deviations from a straight line, the accuracy of the present model is likely to decrease.

EXTENSIONS OF THE PRESENT MODEL

Extensions of the present model may proceed in two principal directions.

ONE STRAIGHT SEGMENT

In this approach, the cable is still approximated by one straight segment. The extensions mentioned below basically extend the applicability of the model to more cases, where the accuracy for each case remains approximately the same.

One extension is to allow the cable to swing out of the vertical plane. This introduces an additional degree of freedom, in the form of an angle coordinate. This would make the model applicable to cases where the towing ship is executing maneuvers involving motions in two horizontal directions, such as towing in a circle. This model may also account for cable strumming since the vortex-induced forces which cause strumming are normal to the plane formed by the cable segment and the relative flow.

In the present model, the lower body is assumed not to rotate. Where the body is fairly large and the cable is not attached to the center of mass of the body, it is important to take rotation of the body into account. This may introduce up to three additional degrees of freedom in the form of three angle coordinates. If the problem is restricted to two dimensions, the number of additional degrees of freedom is one.

The number of additional degrees of freedom depends on the complexity of the system being considered. Each additional degree of freedom introduces an additional

second-order differential equation and also makes existing equations more complex. For example, if one considers the problem of a large body which may rotate in an arbitrary manner being towed by a ship undergoing three-dimensional maneuvers, the number of degrees of freedom is six: two for the inclination of the cable, one for cable stretch, and three for the orientation of the lower body.

SEVERAL SEGMENTS

In this approach, the number of degrees of freedom is increased by representing the actual cable by several segments, each of which may have a different inclination and/or stretch. Perhaps the simplest extension is to allow the model to account for an intermediate body along the cable. In these cases, each of the cables above and below the intermediate body has its own stretch degree of freedom. Thus, an additional degree of freedom, in the form of cable stretch, is introduced. It may be noted that this model is applicable to vibration isolation systems where the motion of the lower body is minimized by the placement of an intermediate body along the cable as well as by varying the spring constant of the cable itself. This is commonly known as a dual isolation system.

The general extension is, of course, to allow each segment to have a different inclination and stretch. This would basically be the segmented cable approach taken in References 5-9. For the two-dimensional problem, each segment has two degrees of freedom. Where the number of segments is small, the modeling of the dynamic and drag characteristics of each cable segment based on the techniques presented in the present study will serve to increase the accuracy of the formulation. As the number of segments increases, the importance of using these careful modeling techniques, of course, decreases.

ACKNOWLEDGMENTS

The author would like to give special thanks to Mr. William E. Smith who suggested and provided encouragement for this work. Mr. Stephen N. Golovato wrote parts of the computer program. Mr. Bruce L. Webster checked the correctness of the differential equations of motion.

REFERENCES

1. Casarella, M.J. and Parsons, M., "A Survey of Investigations on the Configuration and Motion of Cable Systems under Hydrodynamic Loading," Marine Tech. Soc. J., Vol.24, No. 4, pp. 27-44 (Jul-Aug 1970).

2. Schram, J.W., "A Three-Dimensional Analysis of a Towed System," Rutgers University Ph.D. Thesis (Jan 1968).

3. Huffman, R.R., "The Dynamical Behavior of Extensible Cable in a Uniform Flow Field (An Investigation of the Towed Vehicle Problem)," Purdue University Ph.D. Thesis (Jan 1969).

4. Nath, J.H., "Dynamics of Single Point Ocean Moorings of a Buoy - A Numerical Model for Solution by Computer," Oregon State University, Department of Oceanography, Progress Report Reference 69-10 (Jul 1969).

5. Strandhagen, A.G. and Thomas, C.F., "Dynamics of Towed Underwater Vehicles," ASME Winter Annual Meeting, Paper 63-WA-227 (Nov 1963).

6. Walton, T.S. and Polachek, H., "Calculation of Transient Motion of Submerged Cables," Mathematical Tables and Other Aids to Computation, Vol. 14, No. 69, pp. 27-46 (Jan 1960).

7. Polachek, H. et al., "Transient Motion of an Elastic Cable Immersed in a Fluid," Mathematics of Computation, Vol. 17, No. 81, pp. 60-63 (Jan 1963).

8. Froidevaux, M.R. and Scholten, R.A., "Calculation of the Gravity Fall Motion of a Mooring System," Massachusetts Institute of Technology Instrumentation Laboratory Report E-2319 (Aug 1968).

9. Paquette, R.G. and Henderson, B.E., "The Dynamics of Simple Deep-Sea Buoy Moorings," General Motors Defense Research Laboratories, Sea Operations Department, Report 65-79 (Nov 1965).

10. Kerney, K.P., "Small-Perturbation Analysis of Oscillatory Tow-Cable Motion," NSRDC Report 3430 (Nov 1971).

11. Paul, B. and Soler, A.I., "Analysis of Cable Dynamics for Optimum Towing Strategies for Tethered Submersibles," University of Pennsylvania Symposium on Ocean Engineering (Nov 1970).

12. Chey, Y.H., "Hydrodynamics of Launching, Suspension, and Retrieval of Heavy Loads in Deep Ocean Through Cable from Floating Platform in Rough Seas," IEEE Conference on Engineering in the Ocean Environment (Sep 1970).

13. Dale, J.R. et al.,"Dynamic Response of a Suspended Hydrophone to Wave and Flow Effects," ASME Fluids Engineering Conference, Paper 68-FE-39 (May 1968).

14. Timoshenko, S., "Vibration Problems in Engineering," Third Edition, D. Van Nostrand, Princeton, New Jersey (1955), p. 307.

15. Timoshenko, S. and Young, D.H., "Advanced Dynamics," McGraw-Hill, New York (1948), pp.170-171.

16. Lamb, H., "Hydrodynamics," Sixth Edition, Dover Publications, New York (1932), p. 368.

17. Hoerner, S.F., "Fluid-Dynamic Drag," Published by S.F. Hoerner, 148 Busteed Drive, Midland Park, New Jersey (1958), pp. 3-11 to 3-17.

18. Reber, R.K., "The Geometric Configuration and the Towing Tension of a System of Cables of a Mark IV Sweep," Bureau of Ships Report 53 (May 1942), Declassified.

19. Richtmyer, R.D., "Design and Operation of Mark IV Magnetic Mine Sweeping Gear," Bureau of Ships Scientific Group 12 (Jan 1941), Declassified.

20. Wilson, B.W., "Characteristics of Anchor Cables in Uniform Ocean Currents," The A & M College of Texas, Department of Oceanography and Meteorology, Technical Report 204-1 (Apr 1960).

21. Schneider, L. and Nickels, F., Jr., "Cable Equilibrium Trajectory in a Three-Dimensional Flow Field," ASME Winter Annual Meeting, Paper 66-WA/UNT-12 (Nov 1966).

22. Reid, R.O., "Dynamics of Deep-Sea Mooring Lines," Texas A & M University, Department of Oceanography, A & M Project 204, Reference 68-11F (Jul 1968).

✓ 23. Goeller, J.E. and Laura, P.A., "Analytical and Experimental Study of the Dynamic Response of Cable Systems," The Catholic University of America, Department of Mechanical Engineering, Themis Program 893, Report 70-3 (Apr 1970).

✓ 24. Wang, H.T. and Moran, T.L., "Analysis of the Two-Dimensional Steady-State Motion Behavior of Extensible Free-Floating Cable Systems," NSRDC Report 3721 (Oct 1971).

25. Tong, K.N., "Theory of Mechanical Vibration," John Wiley and Sons, New York (1960), pp. 55-56.

INITIAL DISTRIBUTION

Copies

1 Chief of Naval Operations
Attn: OP 1098T6 (Mr. H.Cheng)

1 NAVMAT 0331

5 Commanding Officer
Naval Air Development Center
Johnsville, Warminster, Pa. 18974
Attn: Technical Library (1)
Code AESM (4)

6 Commander
Naval Air Systems Command
Washington, D.C. 20360
Attn: Code 5330 (3)
Code 370 (3)

8 Commander
Naval Ship Systems Command
Department of the Navy
Washington, D.C. 20360
Attn.: Code 0342 (1)
Code 037 (1)
Code 00V (1)
Code 2052 (3)
Code PMS381 (1)
Code 03412 (1)

12 Director
Defense Documentation Center
5010 Duke Street
Alexandria, Virginia 22314

1 Chief of Naval Research
800 N. Quincy
Arlington, Virginia 22217
Attn: Mr. Ralph D. Cooper
Code 438

1 Commander
Naval Facilities Engineering Command
Department of the Navy
Washington, D.C. 20390
Attn: Code 0321

Copies

8 Commander
Naval Ship Engineering Center
Department of the Navy
Center Building
Prince Georges Center
Hyattsville, Maryland 20782
Attn: Code 6110 (1)
Code 6114D (1)
Code 6034B (1)
Code 6136 (1)
Code 6140 (1)
Code 6162 (2)
Code 6144G (1)

1 Naval Ship Engineering Center
Norfolk Division
Boat Engineering Department
Norfolk, Virginia 23511
Attn: Mr. D.L. Blount
Code 6660

2 Officer-in-Charge
Naval Undersea Research & Development Center
3202 E. Foothill Boulevard
Pasadena, California 91107
Attn: Dr. J. Hoyt (1)
Dr. A. Fabula (1)

1 Commander
Naval Electronics Laboratory Center
San Diego, California 92152
Attn: Library

1 Director (Code 2027)
Naval Research Laboratory
Washington, D.C. 20390

Copies

1 Commanding Officer
Navy Underwater Weapons Research and Engineering Station
Newport, Rhode Island 02840

1 Commander
Naval Proving Ground
Dahlgren, Virginia 22448
Attn: Technical Library

1 Commanding Officer and Director
Naval Civil Engineering Laboratory
Port Hueneme, California 93401
Attn: Code L31

1 Commander
Naval Weapons Center (Code 753)
China Lake, California 93555

1 AFFDL (FDDS - Mr. J. Olsen)
Wright-Patterson AFB
Dayton, Ohio 45433

1 NASA Scientific and Technical Information Facility
P.O. Box 33
College Park, Maryland 20740

1 AFORSR (SREM)
1400 Wilson Blvd.
Arlington, Virginia 22209

1 Library of Congress
Science and Technology Division
Washington, D.C. 20540

1 U.S. Coast Guard
1300 E Street, N.W.
Washington, D.C. 20591
Attn: Division of Merchant Marine Safety

1 NOAA
6001 Executive Blvd.
Rockville, Maryland 20852
Attn: Commander R.I. Rybacki

Copies

1 Director
National Bureau of Standards
Washington, D.C. 20234
Attn: Mr. P.S. Klebanoff
Fluid Mechanics Branch

1 Director of Research
National Aeronautics and Space Administration
600 Independence Avenue, S.W.
Washington, D.C. 20546

1 Director
Waterways Experiment Station
Box 631
Vicksburg, Mississippi 39180
Attn: Research Center Library

1 Commander
Naval Ordnance Systems Command
Department of the Navy
Washington, D.C. 20360
Attn: Code ORD-035

1 University of Bridgeport
Bridgeport, Connecticut 06602
Attn: Prof. Earl Uram
Mech. Engr. Dept.

1 Brown University
Providence, Rhode Island 02912
Attn: Div. of Applied Math

1 Naval Architecture Department
College of Engineering
Berkeley, California 94720
Attn: Librarian

3 California Institute of Technology
Pasadena, California 91109
Attn: Dr. A.J. Acosta (1)
Dr. T.Y. Wu (1)
Dr. M.S. Plesset (1)

1 University of Connecticut
Box U-37
Storrs, Connecticut 06268
Attn: Prof. V. Scottron
Hydraulic Research Lab.

Copies

1 Cornell University
Graduate School of Aerospace Engr
Ithaca, New York 14850
Attn: Prof. W.R. Sears

1 Harvard University
2 Divinity Avenue
Cambridge, Massachusetts 02138
Attn: Prof. G. Birkhoff
Dept. of Mathematics

1 Pierce Hall
Harvard University
Cambridge, Massachusetts 02138
Attn: Prof. G.F. Carrier

1 University of Illinois
College of Engineering
Urbana, Illinois 61801
Attn: Dr. J.M. Robertson
Theoretical & Applied
Mechanics Department

1 The University of Iowa
Iowa City, Iowa 52240
Attn: Dr. Hunter Rouse

1 The Johns Hopkins University
Mechanics Department
Baltimore, Maryland 21218
Attn: Prof. O.M. Phillips

2 University of Pennsylvania
The Towne School of Civil and
Mechanical Engineering
Philadelphia, Pennsylvania 19104
Attn: Prof. B. Paul (1)
Prof. A. Soler (1)

1 Kansas State University
Engineering Experiment Station
Seaton Hall
Manhattan, Kansas 66502
Attn: Prof. D.A. Nesmith

Copies

1 Purdue University
Department of Aeronautical
Engineering
Lafayette, Indiana
Attn: Prof. J. Genin

1 University of Kansas
Lawrence, Kansas 60644
Attn: Chm Civil Engr Dept

1 Lehigh University
Bethlehem, Penna. 18015
Attn: Fritz Laboratory Library

1 Long Island University
Graduate Department of Marine
Science
40 Merrick Avenue
East Meadow, N.Y. 11554
Attn: Prof. David Price

1 Massachusetts Institute of
Technology
Hydrodynamics Laboratory
Cambridge, Massachusetts 02139
Attn: Prof. A.T. Ippen

1 Massachusetts Institute of
Technology
Department of Naval Architecture
and Marine Engineering
Cambridge, Massachusetts 02139
Attn: Department Chairman

1 U.S. Merchant Marine Academy
Kings Point, L.I., N.Y. 11204
Attn: Capt. L.S. McCready

1 University of Michigan
Department of Naval Architecture
and Marine Engineering
Ann Arbor, Michigan 48104
Attn: Department Chairman

2 Texas A & M University
Department of Oceanography
College Station, Texas
Attn: Prof. R.O. Reid (1)
Prof. B.W. Wilson (1)

Copies

1 St. Anthony Falls Hydraulic Lab
University of Minnesota
Mississippi River at 3rd Ave.S.E.
Minneapolis, Minnesota 55414
Attn: Director

1 Rutgers University
Department of Mechanical and Aerospace Engineering
New Brunswick, New Jersey 08903
Attn: Prof. S.P. Reyle

2 U.S. Naval Academy
Annapolis, Maryland 21402
Attn: Library (1)
Dr. Bruce Johnson (1)

3 U.S. Naval Postgraduate School
Monterey, California 93940
Attn: Library (1)
Prof. J. Miller (1)
Dr. T. Sarpkaya (1)

1 New York University
University Heights
Bronx, New York 10453
Attn: Prof. W. Pierson, Jr.

2 New York University
Courant Institute of Mathematical Sciences
251 Mercier Street
New York, New York 10012
Attn: Prof. A.S. Peters (1)
Prof. J.J. Stoker (1)

2 University of Notre Dame
Notre Dame, Indiana 46556
Attn: Dr. A. Strandhagen (1)
Dr. J. Nicolaides (1)

1 The Pennsylvania State University
Ordnance Research Laboratory
University Park, Penna. 16801
Attn: Director

Copies

1 Colorado State University
Department of Civil Engineering
Fort Collins, Colorado 80521
Attn: Prof. M. Albertson

1 Aerodynamics Laboratory
Department of Aerospace and Mechanical Sciences
The James Forrestal Research Center
Princeton University
Attn: Prof. G. Mellor

1 Scripps Institution of Oceanography
University of California
La Jolla, California 92038
Attn: J. Pollock

3 Stanford University
Stanford, California 94305
Attn: Prof. H. Ashley (1)
Dept. of Aeronautics and Astronautics
Prof. R. Street (1)
Prof. B. Perry (1)
Dept. Civil Engr

3 Stevens Institute of Technology
Davidson Laboratory
711 Hudson Street
Hoboken, New Jersey 07030
Attn: Dr. J.P. Breslin (1)
Dr. S. Tsakonas (1)
Library (1)

1 University of Texas
Defense Research Laboratory
P.O. Box 8029
Austin, Texas 78712
Attn: Director

1 University of Washington
Applied Physics Laboratory
1013 N.E. 40th Street
Seattle, Washington 98105
Attn: Director

Copies

3 Webb Institute of Naval Architecture
Crescent Beach Road
Glen Cove, L.I., N.Y. 11542
Attn: Prof. E.V. Lewis (1)
Prof. L.W. Ward (1)
Prof. D. Hoffman (1)

2 Catholic University
Institute of Ocean Science and Engineering
620 Michigan Ave., N.E.
Washington, D.C. 20017
Attn: Dr. M. Casarella (2)

2 Oregon State University
Civil Engineering Dept.
Corvallis, Oregon
Attn: Dr. J.H. Nath (1)
Dr. S. Neshyba (1)

1 Worcester Polytechnic Institute
Alden Research Laboratories
Worcester, Massachusetts 01609
Attn: Director

1 Aerojet-General Corporation
1100 W. Hollyvale Street
Azusa, California 91702

1 Bethlehem Steel Corporation
Central Technical Division
Sparrows Point Yard
Sparrows Point, Maryland 21219
Attn: Mr. A. Haff, Technical Mgr

1 Bolt Beranek & Newman, Inc.
1501 Wilson Blvd.
Arlington, Virginia 22209
Attn: Dr. F. Jackson

1 Cornell Aeronautical Laboratory
Applied Mechanics Department
P.O. Box 235
Buffalo, New York 14221

1 Electric Boat Division
General Dynamics Corporation
Groton, Connecticut 06340
Attn: Mr. V. Boatwright, Jr.

Copies

1 Esso International
15 West 51st Street
New York, New York 10019
Attn: Mr. R.J. Taylor, Manager
R & D Tanker Department

1 Westinghouse Ocean Science & Engineering Facility
U.S. Route 50
Annapolis, Maryland

1 General Applied Sciences Laboratories, Inc.
Merrick & Stewart Avenues
Westbury, L.I., New York 11590
Attn: Dr. F. Lane

1 Gibbs & Cox, Inc.
21 West Street
New York, New York 10006
Attn: Technical Library

2 Hydronautics, Inc.
Pindell School Road
Howard County
Laurel, Maryland 20810
Attn: Mr. P. Eisenberg (1)
Mr. M. Tulin (1)

2 McDonnell Douglas Aircraft Co.
Douglas Aircraft Division
3855 Lakewood Boulevard
Long Beach, California 90801
Attn: Mr. John Hess (1)
Mr. A.M.O. Smith (1)

1 Measurement Analysis Corporation
10960 Santa Monica Boulevard
Los Angeles, California 90025

1 National Science Foundation
Engineering Division
1800 G Street, N.W.
Washington, D.C. 20550
Attn: Director

Copies

1 Sperry Rand
Sperry Systems Management Division
7 Aerial Way
Syosset, New York 11791
Attn: Mr. D. Price

1 Newport News Shipbuilding and
Dry Dock Company
4101 Washington Avenue
Newport News, Virginia 23607
Attn: Technical Library Dept.

1 Oceanics, Incorporated
Technical Industrial Park
Plainview, L.I., N.Y. 11803
Attn: Dr. Paul Kaplan

1 Robert Taggart, Inc.
3930 Walnut Street
Fairfax, Virginia 22030
Attn: Mr. R. Taggart

1 Society of Naval Architects and
Marine Engineers
74 Trinity Place
New York, New York 10006

2 Southwest Research Institute
8500 Culebra Road
San Antonio, Texas 78206
Attn: Dr. H. Abramson (1)
Applied Mechanics Review (1)

1 Tracor, Incorporated
6500 Tracor Lane
Austin, Texas 78721

1 Woods Hole Oceanographic
Institute
Woods Hole, Massachusetts 02543
Attn: Reference Room

1 Mr. B.H. Ujihara
North American Aviation, Inc.
Space and Information Systems Div.
12214 Lakewood Boulevard
Downey, California 90241

Copies

1 McKiernan-Terry Division of
Litton Systems, Inc.
580 Winter Ave.
Paramus, N.J. 07652

1 Ocean Science & Engineering, Inc.
Port of Palm Beach
301 Broadway
Riviera Beach, Fla. 33404
Attn: Mr. Robert Snyder

1 Hydrospace Research Corporation
2150 Fields Road
Rockville, Maryland 20850
Attn: Mr. S.M. Gay, Jr.

1 Stanford Research Institute
Menlo Park, California 94025
Attn: Library

1 Cambridge Acoustical Associates, Inc.
129 Mount Auburn Street
Cambridge, Massachusetts 02138
Attn: Dr. M.C. Junger

1 Dr. Roland W. Jeppson
College of Engineering
Utah State University
Logan, Utah 84321

1 Dr. Albert T. Ellis
Department of Applied Mechanics
University of California at
San Diego
P.O. Box 109
La Jolla, California 92038

1 Preformed Line Products Co.
Research & Engineering
5300 St. Clair Ave.
Cleveland, Ohio 44103
Attn: Director

1 Rochester Ropes, Inc.
Culpeper 1, Va.
Attn: Mr. L.A. Rhodes

Copies

1 Samson Cordage Works
Marine Industrial Division
470 Atlantic Ave.
Boston, Mass. 02210

CENTER DISTRIBUTION

Copies	Code	
1	15	
1	152	
1	154	
5	1548	Mr. R. Folb
51	1552	
	1	Mr. J.H. McCarthy
	50	Dr. H.T. Wang
1	156	
1	1576	
1	184	
1	1929	
1	194	

UNCLASSIFIED

Security Classification

DOCUMENT CONTROL DATA - R & D

(Security classification of title, body of abstract and indexing annotation must be entered when the overall report is classified)

1 ORIGINATING ACTIVITY *(Corporate author)*

Naval Ship Research and Development Center
Bethesda, Maryland 20034

2a. REPORT SECURITY CLASSIFICATION

UNCLASSIFIED

2b. GROUP

3 REPORT TITLE

A TWO-DEGREE-OF-FREEDOM MODEL FOR THE TWO-DIMENSIONAL DYNAMIC MOTIONS OF SUSPENDED EXTENSIBLE CABLE SYSTEMS

4 DESCRIPTIVE NOTES *(Type of report and inclusive dates)*

Final Report

5 AUTHOR(S) *(First name, middle initial, last name)*

Henry T. Wang

6. REPORT DATE	7a. TOTAL NO. OF PAGES	7b. NO. OF REFS
October 1971	49	25

8a. CONTRACT OR GRANT NO	9a. ORIGINATOR'S REPORT NUMBER(S)
b. PROJECT NO 5335330/440C/1WZ1400000	3663
c.	9b. OTHER REPORT NO(S) *(Any other numbers that may be assigned this report)*
d.	

10. DISTRIBUTION STATEMENT

APPROVED FOR PUBLIC RELEASE; DISTRIBUTION UNLIMITED

11 SUPPLEMENTARY NOTES	12. SPONSORING MILITARY ACTIVITY
	Naval Air Systems Command Washington, D. C. 20360

13 ABSTRACT

A two-degree-of-freedom nonlinear model is presented for the two-dimensional dynamic motions of an extensible suspended cable system. The two degrees of freedom are the stretch and inclination of the cable. The dynamic and drag characteristics of the cable are carefully modeled. The equations of motion are derived by means of the Lagrange equations. The potential and kinetic energies of the cable are obtained by assuming that the cable stretches uniformly. In order to account for ocean wave particle velocities and current profiles which may vary with depth, the cable may be divided into an arbitrary number of segments to calculate normal and tangential drag. The phenomenon of cable slack is also modeled. A FORTRAN IV computer program, DM2DF, has been written. Numerical results from the program compare favorably with some experimental measurements.

14 KEY WORDS	LINK A		LINK B		LINK C	
	ROLE	WT	ROLE	WT	ROLE	WT
Two-dimensional						
Dynamic motions						
Suspended cable system						
Two degrees of freedom						